



1 **Reduced-complexity air quality intervention modelling**
2 **over China: development of the InMAPv1.6.1-China and**
3 **comparison with the CMAQv5.2 model**

4 Ruili Wu¹, Christopher W. Tessum², Yang Zhang³, Chaopeng Hong⁴, Yixuan Zheng⁵,
5 Qiang Zhang¹

6 ¹Ministry of Education Key Laboratory for Earth System Modelling, Department of Earth System
7 Science, Tsinghua University, Beijing 100084, China

8 ²Department of Civil and Environmental Engineering, University of Illinois at Urbana-Champaign,
9 Urbana, Illinois 61801, United States

10 ³Department of Civil and Environmental Engineering, Northeastern University, Boston, Massachusetts
11 02115, United States

12 ⁴Department of Earth System Science, University of California, Irvine, California 92602, United States

13 ⁵Center of Air Quality Simulation and System Analysis, Chinese Academy of Environmental Planning,
14 Beijing 100012, China

15 *Correspondence to:* Ruili Wu (wurl15@mails.tsinghua.edu.cn)

16 **Abstract.** This paper presents the first development and evaluation of the reduced-complexity air quality
17 model for China. In this study, a reduced-complexity air quality intervention model over China
18 (InMAPv1.6.1-China, hereafter, InMAP-China) is developed by linking a regional air quality model, a
19 reduced-complexity air quality model, an emission inventory database for China, and a health impact
20 assessment model to rapidly estimate the air quality and health impacts of emission sources in China.
21 The modelling system is applied over mainland China for 2017 under various emission scenarios. A
22 comprehensive model evaluation is conducted by comparison against conventional CMAQ simulations
23 and ground-based observations. We found that InMAP-China satisfactorily predicted total PM_{2.5}
24 concentrations in terms of statistical performance. Compared with the observed PM_{2.5} concentrations,
25 the mean bias (MB), normalized mean bias (NMB), and correlations of the total PM_{2.5} concentrations are
26 -8.1 µg/m³, -18%, and 0.6, respectively. The statistical performance is considered to be satisfactory for
27 a reduced-complexity air quality model and remains consistent with that evaluated in the United States.
28 The underestimation of total PM_{2.5} concentrations was mainly caused by its composition, primary PM_{2.5}.
29 In terms of the ability to quantify source contributions of PM_{2.5} concentrations, InMAP-China presents
30 similar results in comparison with those based on the CMAQ model, the difference is mainly caused by



31 the different mechanism and the treatment of secondary inorganic aerosols in the two models. Focusing
32 on the health impacts, the annual $PM_{2.5}$ -related premature mortality estimated using InMAP-China in
33 2017 was 1.92 million, which was 25 ten thousand deaths lower than that estimated based on CMAQ
34 simulations as a result of underestimation of $PM_{2.5}$ concentrations. This work presents a version of the
35 reduced-complexity air quality model over China, provides a powerful tool to rapidly assess the air
36 quality and health impacts associated with control policy, and to quantify the source contribution
37 attributable to many emission sources.

38 **1 Introduction**

39 With rapid urbanization and industrialization, fine particulate matter pollution less than $2.5 \mu m$ in
40 diameter ($PM_{2.5}$) has become a major environmental issue in China. High $PM_{2.5}$ concentrations can be
41 observed over eastern China from satellite observations (Van et al., 2010). Moreover, heavy haze events
42 occurring in metropolises attract the attention of citizens and Chinese governments. $PM_{2.5}$ can affect air
43 quality, ecosystems, and climate change and damage human health through short-term or long-term
44 exposure. The Global Burden of Disease study reported that 1.1 million premature deaths were caused
45 by long-term $PM_{2.5}$ exposure over China in 2015 (Cohen et al., 2017).

46 State-of-the-science three-dimensional air quality models (CTMs) have been widely used in China
47 as tools to simulate regional $PM_{2.5}$ concentrations, quantify the contributions to total $PM_{2.5}$ concentrations
48 resulting from emission sources and assess the benefits associated with control measures (Chang et al.;
49 2019, Li et al., 2015; Zhang et al., 2015; Zhang et al., 2019). The models WRF-CMAQ (Appel et al.,
50 2017; Chang et al., 2019), WRF-Chem (Reddington et al., 2019), WRF-CAMx (Li et al., 2015), and
51 GEOS Chem-adjoint (Zhang et al., 2015) were frequently used in previous studies. To conduct a series
52 of simulations for multiple scenarios or quantify the separate contributions attributable to multiple
53 sources, large computational resources and run time are required while utilizing conventional CTMs. To
54 address this challenges and to improve the availability and accessibility of air quality modelling, a
55 number of reduced-complexity models have been developed by the air quality research community. The
56 three representative reduced-complexity air quality models frequently used are the Estimating Air
57 Pollution Social Impacts Using Regression (EASIUR) model (Heo et al., 2016; Heo et al., 2017), the
58 updated Air Pollution Emission Experiments and Policy (APEEP2) model (Muller et al., 2007; Muller
59 et al., 2011) and the intervention for air pollution (InMAP) model (Tessum et al., 2017). A recent study



60 compares three reduced-complexity models, EASIUR, APEEP2, and InMAP, and the results indicate
61 that these three models are consistent in their assessment of the marginal social cost at the county level
62 (Gilmore et al., 2019). Reduced-complexity air quality models are less computationally intensive and
63 easier to use. However, it is not available for China. Therefore, it is essential to develop a reduced-
64 complexity air quality model over China to quickly predict $PM_{2.5}$ concentrations and the associated health
65 impacts of emission sources.

66 The reduced-complexity intervention model for air pollution, InMAP, was developed by Tessum et
67 al. (Tessum et al., 2017) to rapidly assess the air pollution, health, and economic impacts resulting from
68 marginal changes in air pollutant emissions. Compared with conventional air quality models, InMAP has
69 the advantage of time efficient, can predict annual-average $PM_{2.5}$ concentrations within few hours but
70 with a modest reduction in accuracy compared with CTMs. InMAP reduces the running time by
71 simplifying the physical and chemical process. InMAP has been used to assess marginal health damage
72 of location-specific emission sources (Goodkind et al., 2019), to quantify the health impacts of individual
73 coal-fired power plants in the United States (Thind et al., 2019) and to estimate the health benefits of
74 control policies considering specific locations (Sergi et al., 2020). However, to date, a version of the
75 reduced-complexity air quality intervention model over China is absent.

76 In this work, a reduced-complexity air quality intervention model over China (InMAPv1.6.1-China,
77 hereafter, InMAP-China) is developed on the basis of source code of Intervention Model for Air Pollution
78 model (InMAP) to rapidly predict the air quality and estimate the health impacts of emission sources in
79 China. The modelling system is applied over mainland China for 2017 under various emission scenarios
80 to examine model performance. Comparisons against conventional air quality models and surface
81 observations are performed in this study. The model applicability and limitations are also declared.

82 The paper is organized as follows: Section 2.1 presents the components of InMAP-China includes
83 the interface development between WRF-CMAQ and InMAP to generate parameters of the base
84 atmospheric state, the preprocessing process of emission input data and the exposure-response functions
85 employed in this model. Section 2.2 introduces the evaluation protocol, including the statistical variables
86 adopted and the simulation design in this study. Section 3 presents the evaluation of InMAP-China's
87 predictions of $PM_{2.5}$ air quality and $PM_{2.5}$ -related health impacts in several simulations. Section 4
88 summarizes the conclusions and limitations of this study.



89 **2 Description of InMAPv1.6.1-China model**

90 **2.1 Model components and configurations**

91 The reduced-complexity intervention model for air pollution, InMAP, was developed by Tessum et
92 al. (Tessum et al., 2017) to rapidly assess the air pollution, health, and economic impacts resulting from
93 marginal changes in air pollutant emissions. The model has been widely used in studies (Sergi et al.,
94 2020; Thind et al., 2019; Goodkind et al., 2019; Dimanchevi et al., 2019) focusing on PM_{2.5} pollution
95 and health, economic impacts resulting from emission sources in the United States. In this model, the
96 continuous equation of atmospheric pollutants is solved at an annual scale, and the run time can be
97 reduced. The parameters used to represent physical and chemical processes for simplified simulation are
98 calculated prior to using CTM output data. PM_{2.5} air quality and PM_{2.5}-related premature mortality are
99 predicted and output in the InMAP model.

100 In this work, a Chinese version of the reduced-complexity air quality intervention model InMAP-
101 China is developed for the purpose of rapidly estimating the PM_{2.5} concentration and associated health
102 impacts of emission sources. Figure 1 shows the model framework. Based on the source code of the
103 InMAP model, three-step development work is conducted to establish InMAP-China. Figure 1 shows
104 the model framework. First, we develop a preprocessed interface to calculate physical and chemical
105 process parameters using the WRF-CMAQ output variables to support the simplified simulation in
106 InMAP-China. Second, air pollutant emission data are preprocessed to an appropriate format for the
107 InMAP-China simulation. Third, the exposure-response function of the GEMM model is employed in
108 InMAP-China and replaces the original default function to assess PM_{2.5}-related health impacts.

109 Table 1 presents the basic configurations of InMAP-China. The simulation domain is over East
110 Asia and covers mainland China. The spatial resolution is 36 km. Fourteen vertical layers are used in
111 InMAP-China, ranging from the surface layer to the top level of the tropospheric layer.

112 **2.1.1 Parameter interface development for simplified simulation in InMAP-China**

113 We develop a preprocessed interface to calculate physical and chemical process parameters using
114 WRF-CMAQ output variables for simplified simulation in InMAP-China based on the Environmental
115 Protection Agency's (EPA) work (Baker et al., 2020). The main step of the preprocessed interface
116 includes meteorological and chemical variable extraction and merging, unit conversion, vertical layer
117 mapping, physical and chemical process parameter calculation and average processing. The hourly



118 chemical and meteorological variable outputs from the WRF-CMAQ modelling system are converted
119 into annual-average physical and chemical process parameters required for simplified simulation.

120 A NETCDF file containing the three-dimensional annually averaged parameters to characterize
121 atmospheric advection, dispersion, mixing, chemical reaction, and deposition is generated. Table 2 shows
122 the relationship between the annual-average parameters for simplified simulation and the original hourly
123 variables. In InMAP-China, the annual averaged component and the deviation of wind speed to represent
124 advection are calculated using hourly elements. The offset of wind vectors in different directions may
125 result in some uncertainties in this process. The parameters of eddy diffusion and convective transport
126 are precalculated using hourly elements, including temperature, pressure, boundary layer height, etc. The
127 annual wet deposition rate is determined by the rainwater mixing ratio and cloud fractions. The annual
128 dry deposition rate of particles and gaseous pollutants at the surface level is precalculated using friction
129 speed, heat flux, radiation flux and land cover.

130 The simplification of chemical reactions is different among pollutants. For NO_x , NH_3 , and volatile
131 organic compound (VOC) precursors, annual averaged gas-particle partitioning is adopted and calculated
132 prior to using the output concentrations of species from CMAQ. For SO_2 pollutants, the annual oxidation
133 rate of two major conversion pathways for SO_2 is calculated using concentrations of hydroxyl radical
134 (HO) and hydrogen peroxide (H_2O_2) in CMAQ, and the conversion is estimated in InMAP-China.

135 2.1.2 Prior WRF-CMAQ simulation

136 To generate the meteorological and chemical parameters required by InMAP-China, a one-year
137 WRF-CMAQ simulation is conducted to output hourly meteorological and chemical-related variables in
138 the year 2017. Tables S1 and S2 show the major configurations of the WRF-CMAQ modelling system.
139 The WRF model is driven by the National Centers for Environmental Prediction Final Analysis (NCEP-
140 FNL) (<https://doi.org/10.5065/D6M043C6>) reanalysis data to provide the initial and boundary conditions.
141 The meteorological fields derived from the WRF model is used to drive the CMAQ model (Appel et al.,
142 2016) simulations. The air pollutant emissions used here include anthropogenic emissions over China
143 derived from the MEIC model (<http://meicmodel.org/>), anthropogenic emissions over the region of East
144 Asia outside China derived from the MIX-2010 inventory (Li et al., 2015), and biogenic emissions
145 derived from the MEGANv2.10 model. The CB05 chemical mechanism and the AERO6 aerosol module
146 are employed in the model simulation.

147 Table S3 summarizes the performance statistics of meteorological variables, including surface
148 temperature, relative humidity, and wind speed, in China in 2017, as simulated by the WRF model. The



149 hourly observed data of major meteorological variables derived from the National Climate Data Center
150 (NCDC) are utilized here. The results show that the meteorological variables simulated by the WRF
151 model agree well with the surface observations, which is consistent with previous studies (Wu et al.,
152 2019; Zheng et al., 2015; Hong et al., 2017). The model performs well on the predictions of surface
153 temperature, with an MB of -0.7 K, an NMB of -6.1%, and R of 0.9. The predictions of relative humidity
154 at a height of 2 metres are relatively satisfied with an MB of 4.1% and an NMB of 6.1%. The predictions
155 of wind speed at a height of 10 metres are slightly overestimated, with an MB of 0.3 m/s and an NMB
156 of 12.4%, which may be caused by out-of-date USGS land use data employed in the model runs.

157 The SO₂, NO₂ and PM_{2.5} concentrations modelled across the domain agree well with the surface
158 observations in terms of the statistical performance and monthly variations. Table S4 summarizes the
159 performance of the statistics of major air pollutant concentrations. The nationwide annual averaged PM_{2.5}
160 concentration simulated in 2017 in China was 42.1 µg/m³. Compared with the observed PM_{2.5} of 45.9
161 µg/m³, there are slight underpredictions with an MB of 3.7 µg/m³ and NMB of 8.1%. The CMAQ model
162 has moderate underpredictions of the NO₂ concentrations and SO₂ concentrations, which may be related
163 to the uncertainties of emission inputs. For modelled NO₂ concentrations, MB and NMB are -4.6 µg/m³
164 and -13.9%, respectively. For modelled SO₂ concentrations, MB and NMB are -0.8 µg/m³ and -4.5%,
165 respectively. Figure S3 shows the monthly variation. The variation trend of the observed SO₂, NO₂, and
166 PM_{2.5} concentrations can basically be reproduced in the CMAQ simulations.

167 2.1.3 Preprocessed emission input data

168 Additionally, we develop the preprocessed module to generate vector emission input for the
169 InMAP-China simulation. This module can allocate air pollutant emissions vertically and horizontally to
170 supply the missing parameters for the emission file and convert them into shapefile vector format. The
171 emission data are preprocessed by source and altitude.

172 The anthropogenic emissions of five sectors in China in 2017 from the MEIC inventory
173 (<http://meicmodel.org/>), the anthropogenic emissions over regions outside mainland China in Asia from
174 the MIX-2010 inventory (Li et al., 2015), and the natural emissions estimated using the MEGANv2.10
175 model (Guenther et al., 2012) are employed in this study. Gridded anthropogenic emissions of 0.3
176 degrees for the residential, transportation, and agricultural sectors are preprocessed and input to the
177 surface layer. The gridded air pollutant emissions of the industrial sector and noncoal power plants are
178 preprocessed for allocation to attitudes ranging from 130 metres to 240 metres and 130 metres to 890
179 metres, respectively.



180 The emissions of coal-fired power plants (CPPs) are preprocessed as point sources. The air pollutant
181 emissions and the stack attribution of each unit are provided in the emission file. Because the stack
182 attribution of the power unit is missed in the MEIC inventory, we supplied the information in the
183 preprocessed module based on NEI (National Emission Inventory data) data of power units. For stack
184 height/stack diameter, a linear relationship is first established (see Figure S1), and then, supplementation
185 for these two parameters of Chinese power plants is conducted by using the relationships. The fixed
186 value for the other two variables of stack attribution is set here because the $PM_{2.5}$ concentrations
187 attributable to power plants (CPPs- $PM_{2.5}$) are less sensitive to the two variables (see Figure S2). The
188 stack gas exit velocity and stack gas exit temperature of the power unit are 6 m/s and 313 K, respectively.

189 The air pollutant emissions over regions outside mainland China in Asia and the natural emissions
190 simulated by MEGANv2.10 are preprocessed and input to the surface layer.

191 **2.1.4 Exposure-response function from GEMM**

192 In InMAP-China, we employ the exposure-response function from GEMM to estimate $PM_{2.5}$ -related
193 premature mortality, which was developed by Burnett et al. (Burnett et al., 2018). Premature mortality
194 due to noncommunicable diseases (NCDs) and lower respiratory infections (LRIs) was considered in this
195 study. Mortality is determined by the mortality incidence rate, population, and attributable fraction (AF)
196 to certain $PM_{2.5}$ concentrations. The national mortality incidence rate and the population data were
197 derived from the GBD2017 study (Institute for Health Metrics and Evaluation). The spatial distribution
198 of the population in 2015 from the Gridded Population of World Version 4 (Doxsey et al., 2015) was
199 employed to allocate the population in 2017.

200 **2.2 Evaluation protocol**

201 **2.2.1 Evaluation method**

202 In this study, the performances of the InMAP-China predictions are evaluated by comparison
203 against CMAQ simulations and surface observations. Model-to-model comparison and model-to-
204 observation comparison have both been used to evaluate the performance of reduced-complexity air
205 quality models in previous studies (Tessum et al., 2017, Gilmore et al., 2019).

206 The following aspects are considered to make an evaluation. First, we examine the ability of
207 InMAP-China to predict $PM_{2.5}$ concentrations at different emission levels, which will be introduced in
208 Section 3.1. Moreover, the effects of the model spatial resolution on $PM_{2.5}$ concentration predictions are
209 examined and presented in Section 3.1.3. Second, to examine the ability to quantify source contributions



210 to $PM_{2.5}$ concentrations, we compare the InMAP-China's predictions of the sectoral contributions
211 attributable to power, industry, residential, transportation, and agriculture with those based on the CMAQ
212 model, which will be presented in Section 3.2. Third, focusing on the health impacts, the $PM_{2.5}$ -related
213 premature mortality predicted by InMAP-China is also compared with mortality estimation based on
214 $PM_{2.5}$ exposure derived from CMAQ, which is presented in Section 3.3.

215 The statistical parameters used in this study include the correlation coefficient (R), mean bias (MB),
216 mean error (ME), normalized mean bias (NMB), normalized mean error (NME), and root mean square
217 error (RMSE). The statistical analyses on the performance of InMAP-China are similar to our previous
218 evaluation of conventional CTMs (Zheng et al., 2015; Wu et al., 2019).

219 The annual averaged observed $PM_{2.5}$ concentrations in 2017 were calculated using hourly
220 concentration data from the China National Environmental Monitoring Center, CNEMC
221 (<http://www.cnemc.cn/>). More than 1400 national monitoring sites for air pollutant concentrations are
222 included in the simulation domain.

223 2.2.2 Experimental design

224 We design eleven simulations to examine the model ability of InMAP-China in this study. Table 3
225 shows the sequence of simulations.

226 InMAP_TOT represents the baseline simulation with maximum emissions input, in which five
227 sectoral anthropogenic emissions derived from the MEIC inventory, natural emissions derived from the
228 MEGANv2.10 model, and Asian emissions outside mainland China derived from the MIX-2010
229 inventory are combined as emission inputs. Five sectoral and five abatement simulations are also
230 conducted to examine the ability of InMAP-China to predict concentration changes in response to
231 sectoral emissions and abatement emissions. InMAP-China and CMAQ simulations are both conducted.
232 Correspondingly, eleven CMAQ simulations are performed to make a comparison with the InMAP-
233 China simulations. Due to limited computational resources, each simulation is conducted for four
234 representative months (January, April, July, and October) in 2017.



235 **3 Results and Discussion**

236 **3.1 Model performance of PM_{2.5} concentrations**

237 **3.1.1 Total PM_{2.5} concentrations**

238 Figure 3 shows the performance evaluation of total PM_{2.5} concentrations in the InMAP_TOT
239 simulations. Compared with the observed annual averaged PM_{2.5} concentrations, the total PM_{2.5}
240 concentrations are moderately underpredicted by InMAP-China with an MB of -8.1 μg/m³ and an NMB
241 of -18.1%. Compared with the CMAQ predictions, the total PM_{2.5} concentrations are also underpredicted,
242 with an MB of -5.3 μg/m³ due to the underprediction of primary PM_{2.5}. Consistent air pollutant emissions
243 are employed in the CMAQ and InMAP-China simulations. Therefore, the underpredictions are caused
244 by the different mechanisms in the two models. Basically, InMAP-China reproduces the spatial pattern
245 of total PM_{2.5} concentrations simulated by CMAQ. Notably, significant overpredictions of PM_{2.5}
246 concentrations can be observed over mountain areas across Northern China, and the complex terrain and
247 large emission intensity increase the challenge of predicting PM_{2.5} concentrations using the reduced-
248 complexity air quality model in this region.

249 Figure 4 shows a comparison of PM_{2.5} compositions. Compared with the CMAQ results, the
250 InMAP-China predictions of PM_{2.5} compositions are satisfactory, with NMBs for SO₄²⁻, NO₃⁻, NH₄⁺, and
251 primary PM_{2.5} equal to 13%, -8%, -10%, and -23%, respectively. The predictions of SO₄²⁻, NO₃⁻, and
252 NH₄⁺ perform better than those of primary PM_{2.5}. Figure 5 and Figure 6 compare the spatial distribution
253 of PM_{2.5} compositions, and similar overpredictions of PM_{2.5} compositions can be observed in the
254 mountain area in Northern China.

255 The ability of InMAP-China to predict PM_{2.5} compositions is also examined at various emission
256 levels. Figure 7 compares the concentrations of PM_{2.5} compositions and the proportions of secondary
257 inorganic aerosols (hereafter, SNA) in total PM_{2.5} concentrations in different scenarios by two models.
258 In the InMAP_TOT scenario, the proportion of SNA is 56%, which is extremely close to the 50%
259 proportion in the WRF-CMAQ simulations. In five emission abatement simulations, the proportion was
260 approximately equal to that in the baseline scenario because the linearly treated chemical reaction
261 relationship of SNA was employed in InMAP-China. However, focusing on the simulations of five
262 sectoral emission scenarios, a significant difference can be observed, which is mainly caused by the
263 difference in chemical treatments in InMAP-China and CMAQ. In this situation, the impacts on PM_{2.5}
264 concentrations are distinct due to the nonlinear emission-concentration process.



265 3.1.2 Marginal change in PM_{2.5} concentrations

266 Figure 8 compares the InMAP-China and CMAQ predictions of population-weighted PM_{2.5}
267 concentrations and PM_{2.5} compositions for eleven emission scenarios. Marginal changes in air pollutant
268 concentrations are defined as 1 µg/m³ by normalizing the population-weighted air pollutant
269 concentrations of each scenario using the largest value among all scenarios modelled by CMAQ. The
270 InMAP-China reproduces CMAQ predictions on the marginal change in population-weighted PM_{2.5}
271 concentrations, with a NMB of -12% and correlations of 0.98, as shown in Figure 8(a). This performance
272 is similar to that predicted by InMAP in the United States (Tessum et al., 2017).

273 Figure 8(b)-(f) compares the predictions of PM_{2.5} compositions. The InMAP-China predictions of
274 SO₄²⁻, NO₃⁻, NH₄⁺ and primary PM_{2.5} agree well with the CMAQ results, but the predictions of secondary
275 organic aerosol (SOA) are the poorest. The marginal changes in NO₃⁻ and primary PM_{2.5} concentrations
276 are moderately underpredicted by InMAP-China, with NMB values of -13% and -21%, respectively.
277 Conversely, the marginal change in SO₄²⁻ concentrations is overpredicted with an NMB of 23%. The
278 marginal change in NH₄⁺ predicted by InMAP-China agrees well with the CMAQ predictions. Because
279 few reaction pathways of SOA are included in the CB05 mechanism in the CMAQ simulations, SOAs
280 are underpredicted in the entire modelling system.

281 The regional performance of the changes in PM_{2.5} and its compositions for eleven emission
282 scenarios is also examined in this study. Figures S4-S7 show the regional results. Four regions, including
283 the Beijing-Tianjin-Hebei region (BTH), Yangtze River Delta (YRD), Pearl River Delta (PRD), and Fen
284 Wei Plain (FWP), are analysed here (see Figure 2). At the regional level, the CMAQ predicted marginal
285 changes in population-weighted PM_{2.5} concentrations, and its composition can be reproduced by InMAP-
286 China, which is similar to the nationwide performance. However, the marginal change in SO₄²⁻
287 concentrations over the BTH is significantly overpredicted by InMAP-China, with an NMB of 135%,
288 which is expected to be improved by optimizing the representation of the annual sulfate oxidation rate
289 in this region.

290 3.2 Model performance of source contributions

291 Figure 9 shows the contribution of each sector to PM_{2.5} concentrations nationwide and at the regional
292 scale, and Table 4 displays the proportion value of sectoral contribution based on two models. The
293 predictions of the source contributions of PM_{2.5} concentrations in InMAP-China are basically reliable
294 compared with those based on the CMAQ model, and the difference can be explained.



295 The results based on the two models indicate that the industrial and residential sectors are the first
296 and second contributors among the five sectors. The contribution of the electricity sector is comparable
297 when using the two models, while the contributions of transportation and agriculture are moderately
298 different, which is mainly due to the difference in the model mechanism and the treatment of secondary
299 inorganic aerosols in the two models. At the regional scale, the difference in the sectoral contribution
300 caused by the mechanism in the two models is more significant than at the national scale.

301 **3.3 Model performance of PM_{2.5}-related premature mortality**

302 Figure 10 compares the predictions of PM_{2.5}-related premature mortality based on two models at
303 the provincial level. The PM_{2.5}-related premature mortality estimated using InMAP-China was 1.92
304 million people in 2017. Compared with the CMAQ-based estimations, 25 ten thousand deaths are
305 underpredicted by InMAP-China because of underestimation of total PM_{2.5} concentrations in the baseline
306 simulation. At the provincial level, the PM_{2.5}-related premature mortality in Beijing city, Tianjin city,
307 Hebei province and Shanghai city is slightly overpredicted by InMAP-China, with the relative difference
308 ranging from 4% to 15%. Conversely, for the other majority of provinces, PM_{2.5}-related premature
309 mortality is underpredicted by InMAP-China, with the relative difference ranging from -3% to -44%.

310 **4 Conclusions**

311 This work develops a reduced-complexity air quality intervention model over China and presents a
312 comprehensive evaluation by comparing CMAQ simulations and surface observations. InMAP-China
313 has the advantage of being time-efficient in conducting air quality predictions and health impact
314 assessments of emission sources in China.

315 InMAP-China performed well for the prediction of PM_{2.5} concentrations. The model satisfactorily
316 predicts total PM_{2.5} concentrations in the baseline simulation in terms of statistical performance.
317 Compared with the observed PM_{2.5} concentrations, the MB, NMB, and correlations of the total PM_{2.5}
318 concentrations are -8.1 µg/m³, -18%, and 0.6, respectively. The statistical performance is satisfactory for
319 a reduced-complexity air quality model and remains consistent with the performance evaluation in the
320 United States. The underestimation of total PM_{2.5} mainly comes from the primary PM_{2.5}. Moreover, the
321 spatial pattern of total PM_{2.5} concentrations can be reproduced in InMAP-China, while an overestimation
322 over the mountain area in Northern China can be observed. The large emission intensity and complex
323 terrain over this region increase the difficulty of modelling concentrations in this area. The predictions



324 of source contributions to $PM_{2.5}$ concentrations by InMAP-China are comparable with those based on
325 the CMAQ model, and the difference is mainly caused by the different mechanism and the treatment on
326 secondary inorganic aerosols in two models. Focusing on the predictions of health impacts, InMAP-
327 China shows moderate underpredictions of 25 ten thousand people deaths compared with CMAQ-based
328 predictions due to the underestimation of total $PM_{2.5}$ concentrations.

329 Although the modelling system has an acceptable performance, research work is suggested to
330 further improve the model performance. This study is subject to some limitations and uncertainties. In
331 InMAP-China, the annual-average chemical and physical processes parameters are calculated using
332 hourly parameters from WRF-CMAQ. Complicated seasonal and daily variations affecting the formation
333 and transportation of particulate matter are challenging to retain. The intensity of advection of the air
334 mass is supposed to be weakened due to the offset of the wind vector in the averaging process, which
335 was also pointed out in a previous study. Moreover, InMAP-China has difficulty predicting SOA
336 concentrations because reaction pathways for SOA are insufficient in this modelling system.

337 InMAP-China has the advantage of time efficiency and a satisfactory performance in this study;
338 however, this model has a modest reduction in accuracy compared with conventional CTMs; hence, some
339 limitations still exist for model applications. In terms of the applicability of this modelling system, we
340 recommend users to select InMAP-China as a prior tool with the following objectives: quantification of
341 the contribution of multiple emission sources in baseline atmospheric conditions, for instance, the $PM_{2.5}$
342 air quality and health impacts contributed by individual CPPs; and rapid estimation of the general air
343 quality and health benefits attributable to a series of control policies. Instead, if the objective of
344 simulations is to predict the actual situation and pre-estimate the reductions in $PM_{2.5}$ concentrations due
345 to control measures, conventional CTMs are a better choice because the change in atmospheric
346 conditions along with emission change should be taken into account.

347
348
349
350
351
352
353
354



355 **Code and data availability**

356 The source code of the reduced-complexity air quality model, InMAP, is available at
357 <https://github.com/spatialmodel/inmap>. The source code for the localized version over China
358 (InMAPv1.6.1-China), the data related to this study as well as the user manual are available at
359 <https://doi.org/10.5281/zenodo.4686431>.

360 **Author contributions**

361 RL. Wu and Q. Zhang designed the research and RL. Wu carried them out. RL. Wu, CW. Tessum and
362 Y. Zhang contributed to model development. RL. Wu prepared the manuscript with contributions from
363 all co-authors.

364 **Competing interests**

365 The authors declare no competing interests.

366 **Acknowledgements**

367 This work was supported by the National Natural Science Foundation of China (41921005 and
368 41625020). And this work was also funded under Assistance Agreement No. RD835871 awarded by the
369 U.S. EPA to Yale University. The views expressed in this manuscript are those of the authors alone and
370 do not necessarily reflect the views and policies of the U.S. EPA. The EPA does not endorse any products
371 or commercial services mentioned in this publication.

372 **References**

373 A. Xiu, J. E. Pleim. Development of a Land Surface Model. Part I: Application in a Mesoscale
374 Meteorological Model. *Journal of Applied Meteorology*, 40:192-209, 2011.
375 Appel, K.W., Napelenok, S.L., Hogrefe, C., Foley, K.M., Pouliot, G.A., Murphy, B., Heath, N., Roselle,
376 S., Pleim, J., Bash, J.O., Pye, H.O.T., Mathur, R. Overview and evaluation of the Community Multiscale
377 Air Quality (CMAQ) modelling system version 5.2. *Air Pollution Modelling and its Application XXV*,
378 11:63-72. ITM 2016. Springer Proceedings in Complexity. Springer, Cham, doi: 10.1007/978-3-319-
379 57645-9_11, 2017.



380 Appel, K.W., Napelenok, S.L., Hogrefe, C., Foley, K.M., Pouliot, G.A., Murphy, B., Heath, N., Roselle,
381 S., Pleim, J., Bash, J.O., Pye, H.O.T., Mathur, R. Overview and evaluation of the Community Multiscale
382 Air Quality (CMAQ) modelling system version 5.2. *Air Pollution Modelling and its Application XXV*,
383 11:63-72. ITM 2016. Springer Proceedings in Complexity. Springer, Cham, doi: 10.1007/978-3-319-
384 57645-9_11, 2017.

385 Baker, K. R.; Amend, M.; Penn, S.; Bankert, J.; Simon, H.; Chan, E.; Fann, N.; Zawacki, M.; Davidson,
386 K.; Roman, H., A database for evaluating the InMAP, APEEP, and EASIUR reduced complexity air-
387 quality modelling tools. *Data in Brief*, 28, 2020.

388 Burnett, R.; Chen, H.; Szyszkowicz, M.; Fann, N.; Hubbell, B.; Pope, C. A.; Apte, J. S.; Brauer, M.;
389 Cohen, A.; Weichenthal, S.; Coggins, J.; Di, Q.; Brunekreef, B.; Frostad, J.; Lim, S. S.; Kan, H. D.;
390 Walker, K. D.; Thurston, G. D.; Hayes, R. B.; Lim, C. C.; Turner, M. C.; Jerrett, M.; Krewski, D.; Gapstur,
391 S. M.; Diver, W. R.; Ostro, B.; Goldberg, D.; Crouse, D. L.; Martin, R. V.; Peters, P.; Pinault, L.;
392 Tjepkema, M.; Donkelaar, A.; Villeneuve, P. J.; Miller, A. B.; Yin, P.; Zhou, M. G.; Wang, L. J.; Janssen,
393 N. A. H.; Marra, M.; Atkinson, R. W.; Tsang, H.; Thach, Q.; Cannon, J. B.; Allen, R. T.; Hart, J. E.;
394 Laden, F.; Cesaroni, G.; Forastiere, F.; Weinmayr, G.; Jaensch, A.; Nagel, G.; Concin, H.; Spadaro, J.
395 V., Global estimates of mortality associated with long-term exposure to outdoor fine particulate matter.
396 *Proceedings of the National Academy of Sciences of the United States of America*, 115, (38), 9592-9597,
397 2018.

398 C. J. Walcek, Taylor GR. A Theoretical Method for Computing Vertical Distributions of Acidity and
399 Sulfate Production within Cumulus Clouds. *J. of the Atmos. Sci.* 43:339-55, 1986.

400 Chang, X.; Wang, S.; Zhao, B.; Xing, J.; Liu, X.; Wei, L.; Song, Y.; Wu, W.; Cai, S.; Zheng, H.; Ding,
401 D.; Zheng, M., Contributions of inter-city and regional transport to PM_{2.5} concentrations in the Beijing-
402 Tianjin-Hebei region and its implications on regional joint air pollution control. *Science of the Total*
403 *Environment*, 660, 1191-1200, 2019.

404 Cohen, A. J.; Brauer, M.; Burnett, R.; Anderson, H. R.; Frostad, J.; Estep, K.; Balakrishnan, K.;
405 Brunekreef, B.; Dandona, L.; Dandona, R.; Feigin, V.; Freedman, G.; Hubbell, B.; Jobling, A.; Kan, H.;
406 Knibbs, L.; Liu, Y.; Martin, R.; Morawska, L.; Pope, C. A., III; Shin, H.; Straif, K.; Shaddick, G.; Thomas,
407 M.; van Dingenen, R.; van Donkelaar, A.; Vos, T.; Murray, C. J. L.; Forouzanfar, M. H., Estimates and



408 25-year trends of the global burden of disease attributable to ambient air pollution: an analysis of data
409 from the Global Burden of Diseases Study 2015. *Lancet* 389, (10082), 1907-1918, 2017.

410 Dimanchevi, E. G.; Paltsev, S.; Yuan, M.; Rothenberg, D.; Tessum, C. W.; Marshall, J. D.; Selin, N. E.,
411 Health co-benefits of sub-national renewable energy policy in the US. *Environmental Research Letters*,
412 14, (8), 2019.

413 Doxsey-Whitfield E, MacManus K, Adamo S B, Susana B, Pistoiesi L, Squires J, Borkovska O and
414 Baptista S R Taking advantage of the improved availability of census data: a first look at the gridded
415 population of the world, version 4 *Pap.Appl. Geogr.* 1 226–34, 2015.

416 E. J. Mlawer, S. J. Taubman, P. D. Brown, M. J. Iacono, S. A. Clough. Radiative transfer for
417 inhomogeneous atmospheres: RRTM, a validated correlated-k model for the longwave. *J Geophys Res*,
418 102:16663-82, 1997.

419 Fountoukis C and Nenes A. ISORROPIA II: A Computationally Efficient Aerosol Thermodynamic
420 Equilibrium Model for K^+ , Ca^{2+} , Mg^{2+} , NH_4^+ , Na^+ , SO_4^{2-} , NO_3^- , Cl^- , H_2O Aerosols, *Atmos Chem Phys*,
421 7, 4639-4659, 2007.

422 Gilmore, E. A.; Heo, J.; Muller, N. Z.; Tessum, C. W.; Hill, J. D.; Marshall, J. D.; Adams, P. J., An inter-
423 comparison of the social costs of air quality from reduced-complexity models. *Environmental Research*
424 *Letters*, 14, (7), 2019.

425 Global Burden of Disease Collaborative Network. Global Burden of Disease Study 2017 (GBD 2017)
426 Population Estimates 1950-2017. Seattle, United States: Institute for Health Metrics and Evaluation
427 (IHME), 2018.

428 Global Burden of Disease Collaborative Network. Global Burden of Disease Study 2017 (GBD 2017)
429 Cause-Specific Mortality 1980-2017. Seattle, United States: Institute for Health Metrics and Evaluation
430 (IHME), 2018.

431 Goodkind AL, Tessum CW, Coggins JS, Hill JD, Marshall JD. Fine-scale damage estimates of particulate
432 matter air pollution reveal opportunities for location-specific mitigation of emissions. *Proceedings of the*
433 *National Academy of Sciences*. Apr 3:201816102. <https://doi.org/10.1073/pnas.1816102116>, 2019.

434 Guenther, A. B.; Jiang, X.; Heald, C. L.; Sakulyanontvittaya, T.; Duhl, T.; Emmons, L. K.; Wang, X.,
435 The Model of Emissions of Gases and Aerosols from Nature version 2.1 (MEGAN2.1): an extended and



436 updated framework for modelling biogenic emissions. *Geoscientific Model Development Discussions*, 5,
437 (2), 1503-1560, 2012.

438 Heo, J.; Adams, P. J.; Gao, H. O., Public health costs accounting of inorganic PM_{2.5} pollution in
439 metropolitan areas of the United States using a risk-based source-receptor model. *Environment*
440 *International*, 106, 119-126, 2017.

441 Heo, J.; Adams, P. J.; Gao, H. O., Reduced-form modelling of public health impacts of inorganic PM_{2.5}
442 and precursor emissions. *Atmospheric Environment*, 137, 80-89, 2016.

443 Hong, C.; Zhang, Q.; Zhang, Y.; Tang, Y.; Tong, D.; He, K., Multi-year downscaling application of
444 two-way coupled WRF v3.4 and CMAQ v5.0.2 over east Asia for regional climate and air quality
445 modelling: model evaluation and aerosol direct effects. *Geoscientific Model Development*, 10, (6),
446 2447-2470, 2017.

447 J. E. Pleim. A Combined Local and Nonlocal Closure Model for the Atmospheric Boundary Layer. Part
448 I: Model Description and Testing. *J. Appl. Meteorol. Clim*, 46:1383-95, 2007.

449 J. S. Chang, R. A. Brost, I. S. A. Isaksen, S. Madronich, P. Middleton, W. R. Stockwell, et al. A three-
450 dimensional Eulerian acid deposition model: Physical concepts and formulation. *J Geophys. Res*,
451 92:14681-700, 1987.

452 J. S. Kain. The Kain-Fritsch Convective Parameterization: An Update. *J. of Appl. Meteorol.* 2004,
453 43:170-81.

454 Li, M.; Zhang, Q.; Kurokawa, J.-i.; Woo, J.-H.; He, K.; Lu, Z.; Ohara, T.; Song, Y.; Streets, D. G.;
455 Carmichael, G. R.; Cheng, Y.; Hong, C.; Huo, H.; Jiang, X.; Kang, S.; Liu, F.; Su, H.; Zheng, B., MIX:
456 a mosaic Asian anthropogenic emission inventory under the international collaboration framework of the
457 MICS-Asia and HTAP. *Atmospheric Chemistry and Physics*, 17, (2), 935-963, 2017.

458 Li, X.; Zhang, Q.; Zhang, Y.; Zheng, B.; Wang, K.; Chen, Y.; Wallington, T. J.; Han, W.; Shen, W.; Zhang,
459 X.; He, K., Source contributions of urban PM_{2.5} in the Beijing-Tianjin-Hebei region: Changes between
460 2006 and 2013 and relative impacts of emissions and meteorology. *Atmospheric Environment*, 123, 229-
461 239, 2015.

462 Liu, F.; Zhang, Q.; Tong, D.; Zheng, B.; Li, M.; Huo, H.; He, K. B., High-resolution inventory of
463 technologies, activities, and emissions of coal-fired power plants in China from 1990 to 2010.



464 Atmospheric Chemistry and Physics, 15, (23), 13299-13317, 2015.

465 M.-D. Chou, M. J. Suarez, C.-H. Ho, M. M.-H. Yan, K.-T. Lee. Parameterizations for Cloud Overlapping
466 and Shortwave Single-Scattering Properties for Use in General Circulation and Cloud Ensemble Models.
467 J. of Climate, 11:202-14, 1998.

468 Muller, N. Z., Mendelsohn, R. Measuring the damages of air pollution in the United States. Journal of
469 Environmental Economics and Management, 54(1), 1–14. <https://doi.org/10.1016/j.jeem.2006.12.002>,

470 Muller, N. Z., Mendelsohn, R., & Nordhaus, W. Environmental accounting for pollution in the United
471 States economy. American Economic Review, 101(5), 1649-75. DOI:10.1257/aer.101.5.1649, 2011.

472 Multi-resolution Emission Inventory of China (<http://meicmodel.org/>).

473 National Centers for Environmental Prediction/National Weather Service/NOAA/US Department of
474 Commerce NCEP FNL Operational Model Global Tropospheric Analyses, continuing from July 1999
475 Dataset (<https://doi.org/10.5065/D6M043C6>), 2000.

476 Reddington, C. L.; Conibear, L.; Knote, C.; Silver, B.; Li, Y. J.; Chan, C. K.; Arnold, S. R.; Spracklen,
477 D. V., Exploring the impacts of anthropogenic emission sectors on PM_{2.5} and human health in South and
478 East Asia. Atmospheric Chemistry and Physics, 19, (18), 11887-11910, 2019.

479 Sergi, B. J.; Adams, P. J.; Muller, N. Z.; Robinson, A. L.; Davis, S. J.; Marshall, J. D.; Azevedo, I. L.,
480 Optimizing Emissions Reductions from the U.S. Power Sector for Climate and Health Benefits.
481 Environmental science & technology, 54, (12), 7513-7523, 2020.

482 Skamarock W, Klemp J, Dudhia J, Gill D, Barker D, Duda M, Huang X, Wang Wand Powers J A
483 description of the Advanced Research WRF Version 3 NCAR technical note (Boulder, CO: National
484 Center for Atmospheric Research), 2008.

485 Tessum, C. W.; Hill, J. D.; Marshall, J. D., InMAP: A model for air pollution interventions. PLoS One,
486 12, (4), e0176131, 2017.

487 Thind, M. P. S.; Tessum, C. W.; Azevedo, I. L.; Marshall, J. D., Fine Particulate Air Pollution from
488 Electricity Generation in the US: Health Impacts by Race, Income, and Geography. Environmental
489 Science & Technology, 53, (23), 14010-14019, 2019.

490 United States Environmental Protection Agency. National Emission Inventory data.
491 <https://www.epa.gov/air-emissions-inventories/2011-national-emissions-inventory-nei-data>. 2011.



492 van Donkelaar, A.; Martin, R. V.; Brauer, M.; Hsu, N. C.; Kahn, R. A.; Levy, R. C.; Lyapustin, A.; Sayer,
493 A. M.; Winker, D. M., Global Estimates of Fine Particulate Matter using a Combined Geophysical-
494 Statistical Method with Information from Satellites, Models, and Monitors. *Environmental Science &*
495 *Technology*, 50, (7), 3762-3772, 2016.

496 Whitten G Z, Heo G, Kimura Y, et al. A new condensed toluene mechanism for Carbon Bond CB05-TU.
497 *Atmos. Environ*, 44(40SI):5346-5355, 2010.

498 Wu, R.; Liu, F.; Tong, D.; Zheng, Y.; Lei, Y.; Hong, C.; Li, M.; Liu, J.; Zheng, B.; Bo, Y.; Chen, X.; Li,
499 X.; Zhang, Q., Air quality and health benefits of China's emission control policies on coal-fired power
500 plants during 2005–2020. *Environmental Research Letters*, 14, (9), 094016, 2019.

501 Zhang, L.; Liu, L. C.; Zhao, Y. H.; Gong, S. L.; Zhang, X. Y.; Henze, D. K.; Capps, S. L.; Fu, T. M.;
502 Zhang, Q.; Wang, Y. X., Source attribution of particulate matter pollution over North China with the
503 adjoint method. *Environmental Research Letters*, 10, (8), 2015.

504 Zhang, Q.; Zheng, Y.; Tong, D.; Shao, M.; Wang, S.; Zhang, Y.; Xu, X.; Wang, J.; He, H.; Liu, W.; Ding,
505 Y.; Lei, Y.; Li, J.; Wang, Z.; Zhang, X.; Wang, Y.; Cheng, J.; Liu, Y.; Shi, Q.; Yan, L.; Geng, G.; Hong,
506 C.; Li, M.; Liu, F.; Zheng, B.; Cao, J.; Ding, A.; Gao, J.; Fu, Q.; Huo, J.; Liu, B.; Liu, Z.; Yang, F.; He,
507 K.; Hao, J., Drivers of improved PM_{2.5} air quality in China from 2013 to 2017. *Proceedings of the*
508 *National Academy of Sciences of the United States of America*, 116, (49), 24463-24469, 2019.

509 Zheng, B.; Zhang, Q.; Zhang, Y.; He, K. B.; Wang, K.; Zheng, G. J.; Duan, F. K.; Ma, Y. L.; Kimoto, T.,
510 Heterogeneous chemistry: a mechanism missing in current models to explain secondary inorganic aerosol
511 formation during the January 2013 haze episode in North China. *Atmospheric Chemistry and Physics*,
512 15, (4), 2031-2049, 2015.

513
514
515
516
517
518
519



520 **Table 1. Model configurations in InMAP-China.**

Category	Parameters	Configurations
Basic	Research area and period	China, 2017
	Spatial resolution	36 km × 36 km
	Vertical layers	14 layers
	Run type	Steady run
	Variable grid	Static grid
	Projection	Lambert
	Grid numbers	305816
	Meteorological and chemical parameters	Calculated using variables from WRFv3.8-CMAQv5.2
Input	Anthropogenic emissions	MEIC, MIX, MEGAN
	Population data	GPW 2015 and GBD 2017
	Baseline mortality rate	GBD 2017
Output	Air pollutants	PM _{2.5} and its composition concentrations
	Mortality	PM _{2.5} -related premature mortality

521

522

523

524

525

526

527

528

529



530 **Table 2 The relationship between parameters for simplified simulation and original variables.**

WRF-CMAQ's Variables		InMAP-China's Parameters	
Variables	Descriptions		Descriptions
		UAvg, UDeviation	
U, V, W	Wind fields	VAvg, VDeviation	Advection and mixing coefficients
		WAvg, WDeviation	
PH, PHB	Base state of geopotential and perturbation geopotential	Dz	Layer heights
PBLH	Planetary boundary layer height	M2d, M2u, Kxxyy, Kzz	Mixing coefficients
T	Potential Temperature	SO ₂ Oxidation, PlumeHeight	Chemical reaction rates and plume rise
P, PB	Base state pressure plus perturbation pressure		Chemical reaction rates and plume rise
QRAIN	Mixing ratio of rain	ParticleWetdep, GasWetdep, SO ₂ Oxidation	Wet deposition Aqueous-phase chemical reaction rates
QCLOUD	Cloud mixing ratio		
CLDFRA	Fraction of grid cell covered by clouds	ParticleWetdep, GasWetdep	Wet deposition
SWDOW	Downward shortwave and longwave radiative flux at ground level	GasDrydep, ParticleWetdep	Dry deposition
N, GLW		M2d, M2u, Kxxyy, Kzz, Drydep	Mixing and dry deposition
HFX	Surface heat flux		Mixing and dry deposition
UST	Friction velocity		
LU_INDE		M2d, M2u, Kxxyy, Kzz	Mixing and convert between mixing ratio and mass concentration
X	Land use type		
DENS	Inverse air density		
aVOC	Anthropogenic VOCs that are SOA precursors	aOrgPartitioning	VOCs/SOA partitioning
aSOA	Anthropogenic SOA		
OH, H ₂ O ₂	Hydroxyl radical and hydrogen peroxide concentrations	SO ₂ Oxidation	Oxidation rates
pNO	ANO ₃ I, ANO ₃ J	NOPartitioning	



				NO _x	/pNO ₃
				partitioning	
gNO	NO and NO ₂				
pNH	ANH ₄ I, ANH ₄ J		NHPartitioning		
					NH ₃ /pNH ₄
gNH	NH ₃				partitioning

531

532

533

534

535

536

537

538

539

540

541

542

543

544

545

546

547

548

549

550

551

552

553

554



555 **Table 3 Simulation experiments conducted using InMAP-China.**

Class	Simulations	Emission input	Physical and chemical parameter input
Sec1	InMAP_POW	Power plants emissions	
Sec2	InMAP_INDUS	Industrial emissions	
Sec3	InMAP_TRANS	Transportation emissions	
Sec4	InMAP_RESI	Residential emissions	
Sec5	InMAP_AGRI	Agricultural emissions	
BASE	InMAP_TOT	Five sectoral anthropogenic emissions and natural emissions	
Aba1	InMAP_RE10	Reduce the air pollutants emissions by 10% based on InMAP_TOT emissions	Converted using WRF-CMAQ simulation data in the year of 2017; Remain the same in all simulations.
Aba2	InMAP_RE30	Reduce the air pollutants emissions by 30% based on InMAP_TOT emissions	
Aba3	InMAP_RE50	Reduce the air pollutants emissions by 50% based on InMAP_TOT emissions	
Aba4	InMAP_RE70	Reduce the air pollutants emissions by 70% based on InMAP_TOT emissions	
Aba5	InMAP_RE90	Reduce the air pollutants emissions by 90% based on InMAP_TOT emissions	

556

557

558

559

560

561

562

563

564



565 **Table 4 Comparison of the proportions of sectoral contributions to PM_{2.5} concentrations using InMAP-**

566 **China and CMAQ.**

Sector	National		BTH		YRD		PRD		FWPY	
	InMA		InMA		InMA		InMA		InMA	
	CMAQ	P-China	CMAQ	P-China	CMAQ	P-China	CMAQ	P-China	CMAQ	P-China
Power	6.9%	8.1%	6.2%	9.4%	7.4%	8.6%	10.4%	8.2%	7.0%	10.0%
	30.8		30.2		33.3		37.5		27.7	
Industry	%	35.0%	%	38.2%	%	39.1%	%	35.4%	%	31.9%
	25.9		24.7		17.9		19.5		30.0	
Residential	%	28.1%	%	28.2%	%	20.8%	%	28.4%	%	33.8%
Transportation	14.0		13.4		15.7		17.1		13.2	
	%	17.3%	%	15.6%	%	21.2%	%	17.5%	%	15.0%
	22.5		25.5		25.7		15.4		22.0	
Agriculture	%	11.5%	%	10.4%	%	12.4%	%	11.6%	%	9.4%

567

568

569

570

571

572

573

574

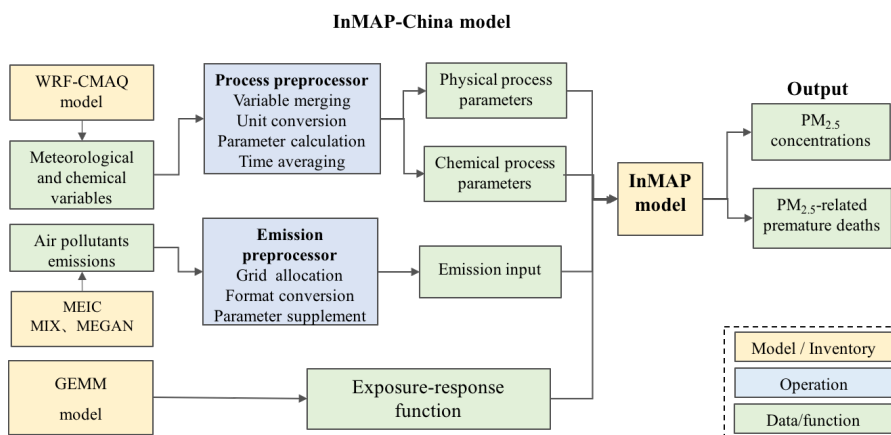
575

576

577

578

579



580

581

Figure 1 Model framework of InMAPv1.6.1-China.

582

583

584

585

586

587

588

589

590

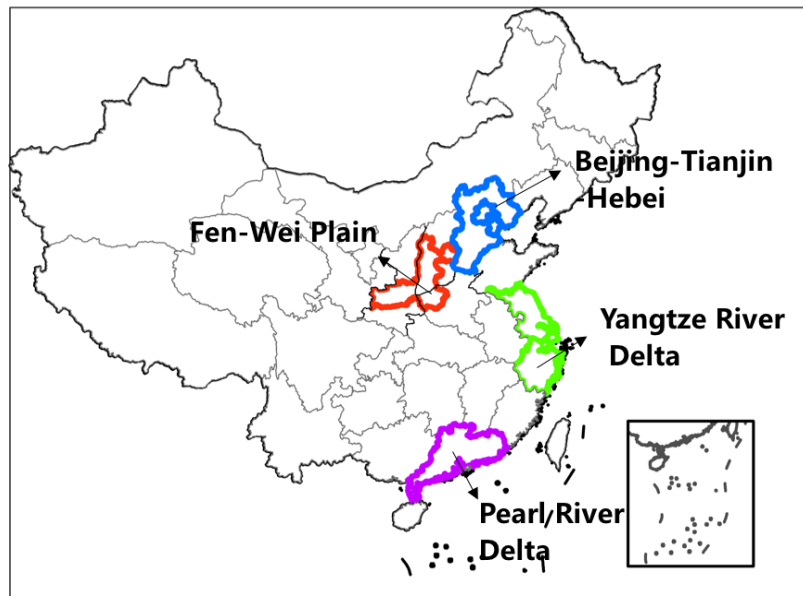
591

592

593

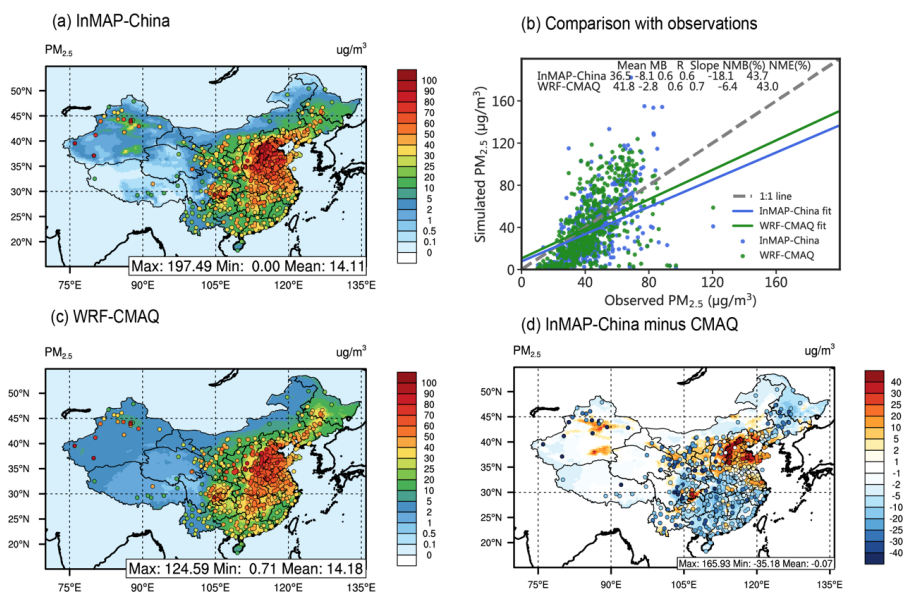
594

595



596
597 **Figure 2** Four key regions defined in this study, including the Beijing-Tianjin-Hebei region, Yangtze River
598 Delta region, Pearl River Delta region and Fen Wei Plain region.

599
600
601
602
603
604
605
606



607

608

609

610

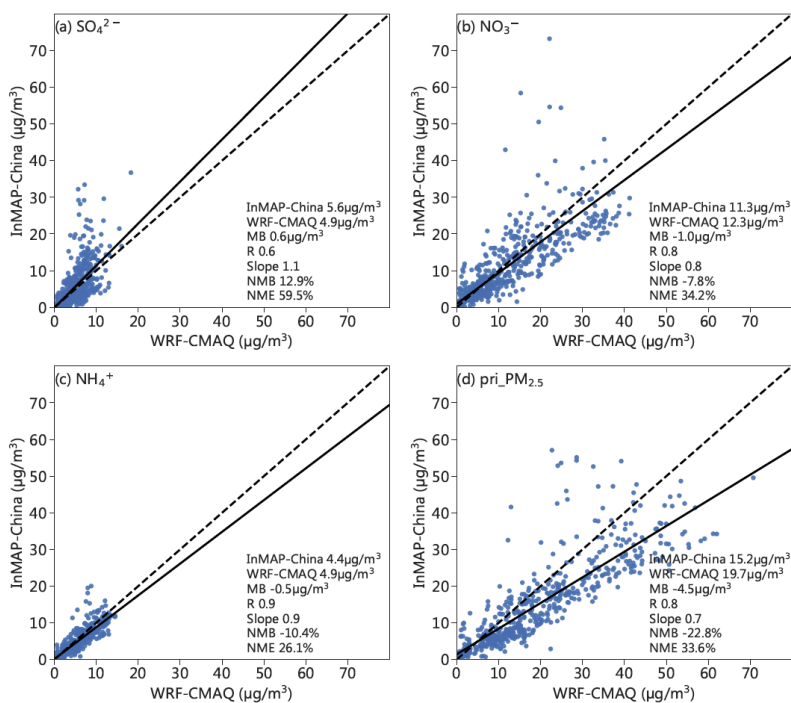
611

612

613

614

Figure 3 The spatial pattern and statistical metrics of total $PM_{2.5}$ concentrations predicted by InMAP-China and WRF-CMAQ. Panels (a) and (c) display the spatial patterns of total $PM_{2.5}$ concentrations predicted by InMAP-China and WRF-CMAQ, respectively. Panel (d) presents the difference in the spatial distribution of the total $PM_{2.5}$ concentrations predicted by the two models. Panel (b) shows the statistical metrics between the simulated and observed $PM_{2.5}$. The observed total $PM_{2.5}$ concentrations are marked as circles in panel (a) and panel (c). In panel (d), the circle shows the difference between the $PM_{2.5}$ simulated by InMAP-China and the observed $PM_{2.5}$. The same colorbar is utilized in the contour and the marked circle.

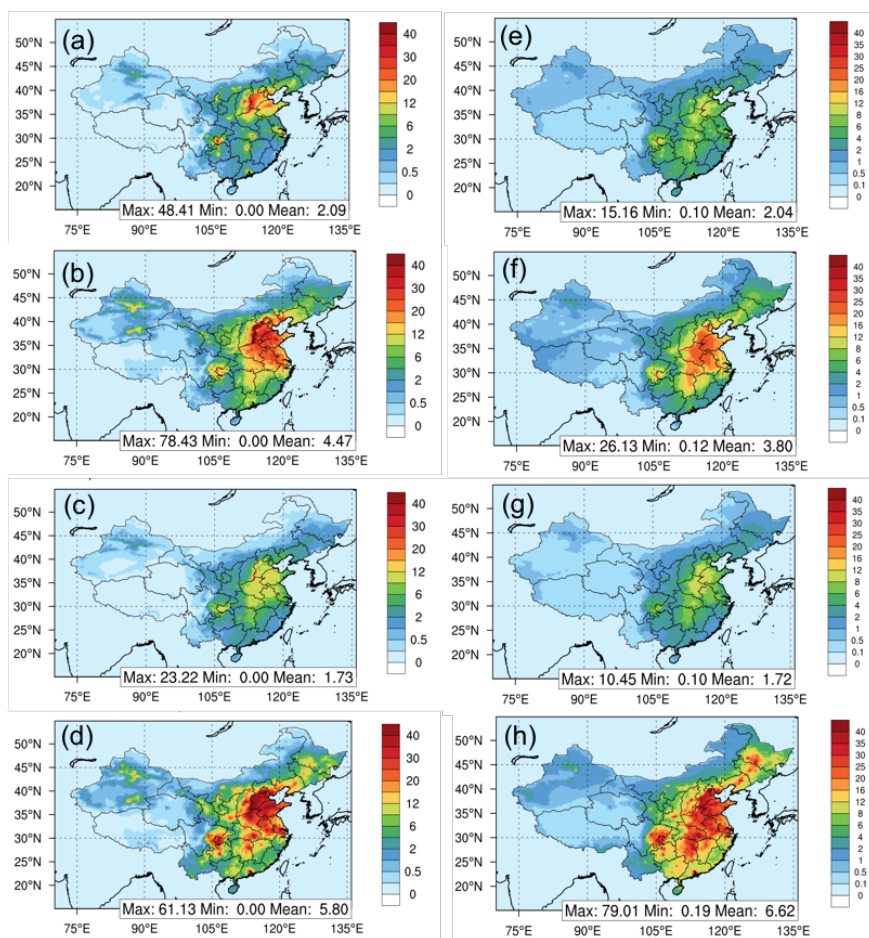


615

616 **Figure 4** Scatter plot comparing the PM_{2.5} composition concentration modelled by the InMAP-China and

617 **WRF-CMAQ** models. Panels (a), (b), (c) and (d) display sulfate, nitrate, ammonium, and primary PM_{2.5},

618 respectively. The statistical metrics are labelled in the lower right corner in each panel.

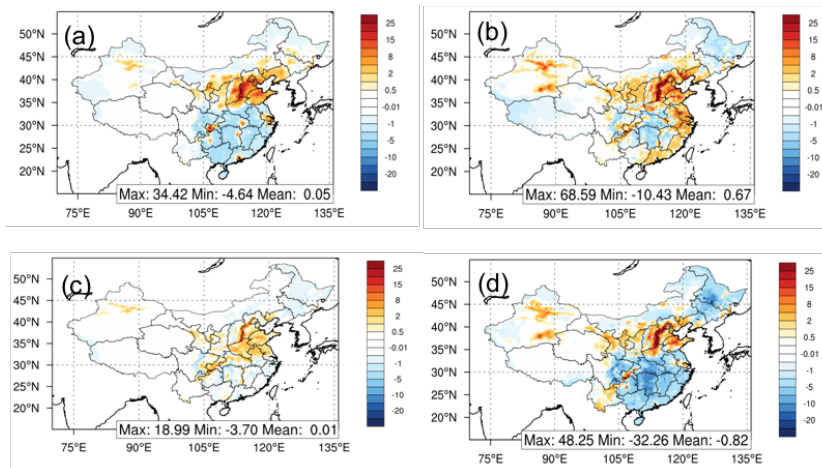


619

620 **Figure 5** The spatial pattern of PM_{2.5} compositions modelled by the InMAP-China and WRF-CMAQ models.

621 Panels (a), (b), (c), and (d) present the sulfate, nitrate, ammonium, and primary PM_{2.5}, respectively, simulated by

622 InMAP-China in the InMAP-TOT scenario. Panels (e), (f), (g), and (h) present the results modelled by WRF-CMAQ.



623

624 **Figure 6** The difference in the spatial pattern of $PM_{2.5}$ compositions between InMAP-China and WRF-CMAQ.

625 Panels (a), (b), (c), and (d) display sulfate, nitrate, ammonium, and primary $PM_{2.5}$, respectively.

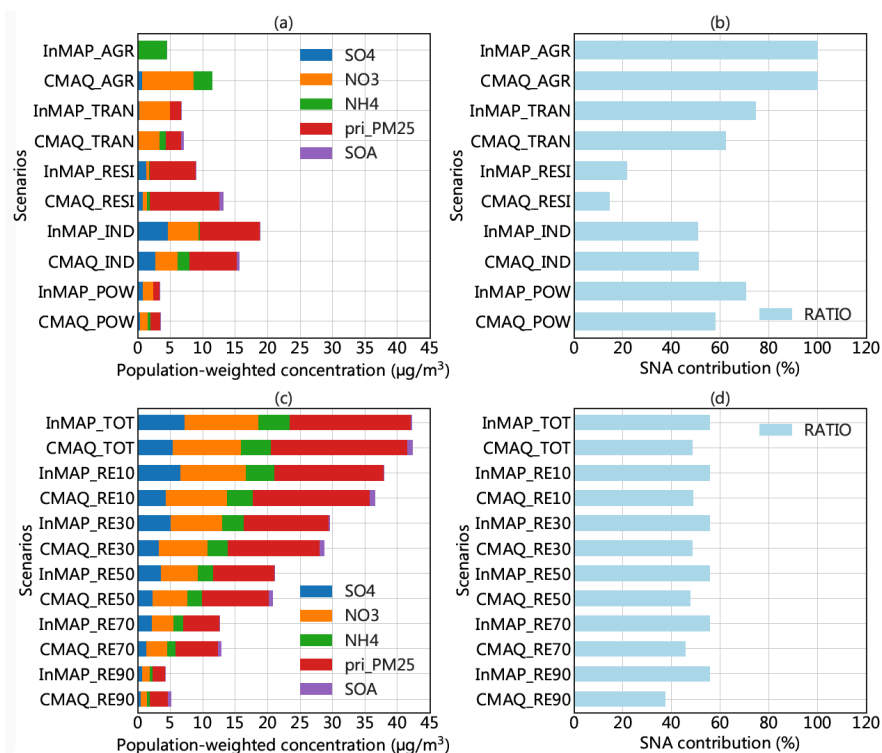
626

627

628

629

630



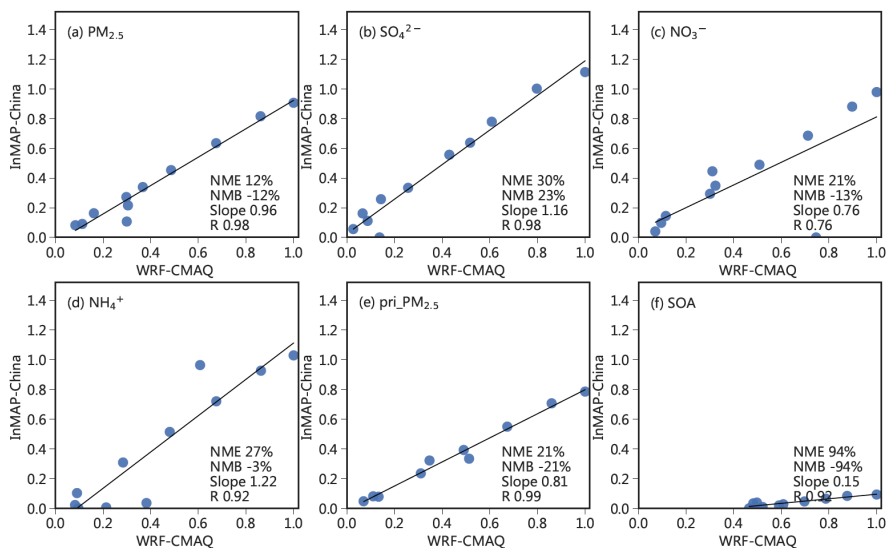
631

632 **Figure 7 Comparison of PM_{2.5} component concentrations and SNA contributions in these eleven simulations.**

633 (a) and (c) show the modelled PM_{2.5} compositions. Panel (a) presents the results of sectoral emission scenarios, and

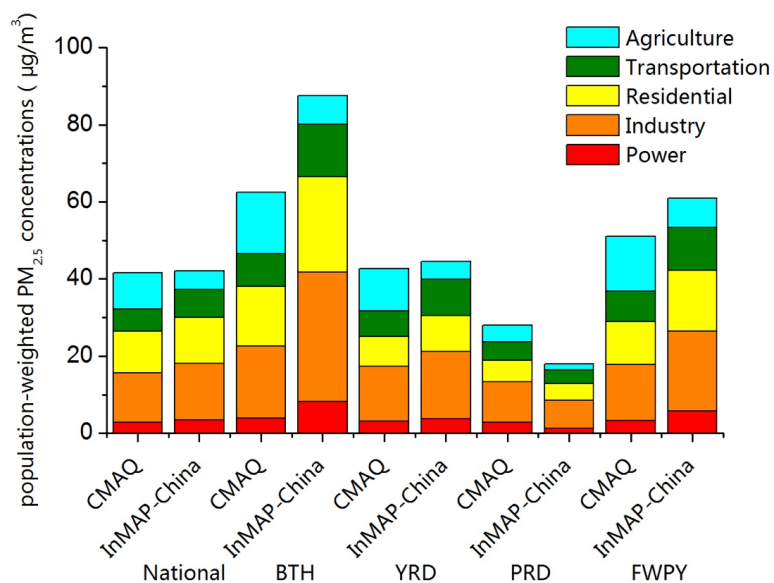
634 panel (c) presents the results of the baseline and emission abatement scenarios. Panels (b) and (d) present the SNA

635 contribution (%) for each scenario.



636
637 **Figure 8** Marginal change in nationwide annual average population-weighted PM_{2.5} concentration and its
638 composition as modelled by InMAP-China and WRF-CMAQ for eleven emissions scenarios. The population-
639 weighted pollutant concentration for each scenario is normalized using the largest value among all scenarios
640 modelled by CMAQ. The eleven dots represent the eleven scenarios, and the statistical metrics are labelled in the
641 lower right corner for each panel.

642
643
644



645

646

647

Figure 9 Comparison of source contributions to population-weighted PM_{2.5} concentrations estimated by the two models.

648

649

650

651

652

653

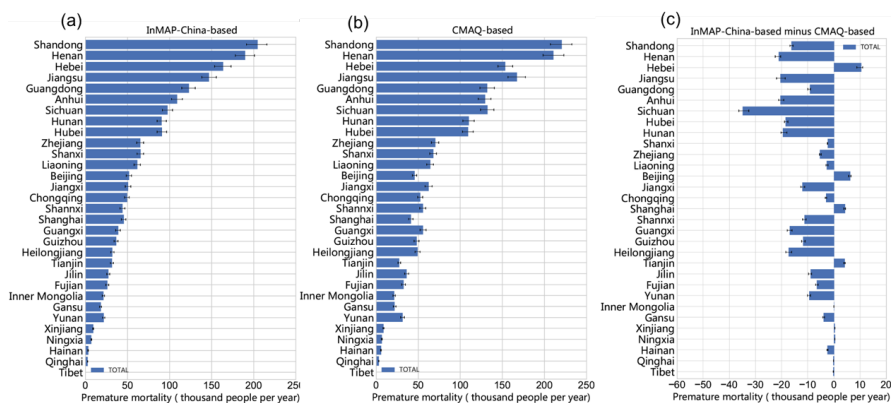
654

655

656

657

658



659

660

Figure 10 Comparison of $PM_{2.5}$ -related premature mortality based on two models. (a) InMAP-China-based;

661

(b) CMAQ-based; and (c) difference between the two model

662

663

664

665

666

667

668

669

670

671

672

673

674

675

676

677